Journal of Alloys and Compounds 500 (2010) 30–33

Contents lists available at ScienceDirect

Journal of Alloys and Compounds

journal homepage: www.elsevier.com/locate/jallcom

Production of a nanocrystalline Ni_3Al-based alloy using mechanical alloying

Masoud Nazarian Samani[a,b,*], Ali Shokuhfar[a], Ali Reza Kamali[b], Morteza Hadi[b]

[a] Faculty of Mechanical Engineering, K.N. Toosi University of Technology, Tehran, Iran
[b] Department of Materials Science and Engineering, Malek Ashtar University of Technology, Shahin Shahr, Iran

ARTICLE INFO

Article history:
Received 13 July 2008
Received in revised form 25 February 2009
Accepted 26 February 2009
Available online 13 March 2009

Keywords:
Ni_3Al-based alloy
Mechanical alloying
Nanostructured materials
Hot pressing

ABSTRACT

A new Ni_3Al-based alloy has been successfully made via densification of mechanically alloyed powders with nominal compositions of Ni–8.14Al–7.83Cr–1.45Mo–0.01B (wt%). Mechanical alloying (MA) was carried out in a planetary ball mill under different conditions. The effect of MA on the structure of elemental powders was investigated. A Ni-based solid solution was produced after 10 h of milling that transformed to a disordered Ni_3Al intermetallic compound with nanocrystalline structure on further milling. The rate of this transformation depended on milling variables such as mill rotation speed and milling media. The yield strength of produced alloy increased with increasing temperature up to 600 °C beyond which it decreased.

1. Introduction

Ni_3Al-based alloys are well known for their excellent high temperature properties such as good mechanical strength, positive temperature coefficient of flow stress, attractive oxidation, creep resistance and alloy design flexibility. The most attractive property of Ni_3Al is that its yield strength increases with increasing temperature up to about 800 °C [1–3]. Poly-crystalline Ni_3Al is a brittle material at room temperature [1,4] and has poor strength and creep properties at high temperatures [5,6]. A number of Ni_3Al-based alloys have been designed to overcome these limitations. In these alloys, the third element is used to enhance the mechanical properties. Boron is added as the key trace addition since it improves the grain boundary cohesive strength and room temperature ductility. The other alloying additions include Cr for reducing environmental embrittlement and oxidation at higher temperatures, Mo for increasing strength at ambient and elevated temperatures, and Zr for reducing solidification shrinkage and macroporosity through the formation of γ+Ni_5Zr as a low melting point (1170 °C) eutectic phase [3].

Ni_3Al-based alloys, especially the well known alloy of IC-221M, are produced by melting and casting processes [6–12]. The major problem in production of these alloys via melting processes is the strong tendency of aluminum to oxidize at elevated temperatures and metal-ceramic interaction during the melting [6,10,12]. On the other hand, the presence of 1.7 wt% Zr in the IC-221M alloy leads to the formation of γ+Ni_5Zr eutectic phase [9]. Ni_5Zr segregates in grain boundaries and hardly dissolves in the alloy [13]. In addition, it limits the hot working of IC-221M. One approach to overcome these problems is to produce the Ni_3Al-based alloys in their net shape by a powder metallurgy process as there is no melting step in these processes. Therefore, Zr can be removed from the chemical composition of the alloy.

In this research, a new alloy with nominal compositions of Ni–8.14Al–7.83Cr–1.45Mo–0.01B (wt%) was produced by mechanical alloying and hot pressing processes. The effects of process variables such as milling media (wet or dry milling) and milling speed on the kinetics of the MA process were also investigated.

2. Experimental

2.1. Materials and procedures

Elemental high purity Ni, B, Cr, Mo and Al powders with an average particle size of 10 μm were mixed to give the nominal compositions of Ni–8.14Al–7.83Cr–1.45Mo–0.01B (wt%). MA was performed for different milling times at room temperature using a Fritsch P6 planetary ball mill under Ar atmosphere. The powder and the stainless steel milling balls were sealed in a stainless steel vial. The ball-to-powder weight ratio was 10:1. MA was carried out under three different milling conditions, series I–III in Table 1. Samples were taken at selected time intervals and characterized by X-ray diffraction (XRD) in a Seifert 3003TT diffractometer using filtered Cu Kα radiation (λ = 0.15406 nm) at 40 kV and 30 mA. Energy-dispersive X-ray spectroscopy (EDX) coupled with the "Vega©Tescan" scanning electron microscope (SEM) was used for the semiquantitative examination of microstructure. The lattice parameters, the mean crystallite size and the mean lattice strain (the latter two determined by the Williamson–Hall method) were calculated from the XRD data taking into account Cu Kα radiation.

A hot pressing machine (model ASTRO HP-20-4560) was used for densification of mechanically alloyed powders. Densification was carried out in a graphite mold under a pressure of 6 MPa at a temperature of 1,000 °C for 10 min. The compressive

* Corresponding author. Tel.: +98 912 7085285; fax: +98 312 5228530.
E-mail address: Masoud.Nazarian@gmail.com (M. Nazarian Samani).

0925-8388/$ – see front matter © 2009 Elsevier B.V. All rights reserved.
doi:10.1016/j.jallcom.2009.02.140

Table 1
Mechanical alloying conditions.

Series	Rotation speed (rpm)	Milling media
I	300	Hexane
II	150	Hexane
III	300	–

tests were carried out on cylinder samples (D: 4 mm, L: 6 mm) at room, 300, 600 and 700 °C using an Instron model 8503 tensile/compressive testing machine at a strain rate of 10^{-2} s^{-1}. Elevated temperature compressive tests were performed in air taking about 20 min to equilibrate the specimens at the relevant temperature in order to complete the test. Hardness measurements were conducted using a Koopa model UV1 machine. Density of materials was measured using Archimedes method.

2.2. Determination of mean crystallite size and mean lattice strain

The Williamson–Hall method was used for calculating the mean crystallite size and mean lattice strain, from the XRD data. In the Williamson–Hall method, the modified Scherrer's equation can be written as follow [14]:

$$B\cos\theta = \frac{0.9\lambda}{d} + e\sin\theta \quad (1)$$

$$B = \sqrt{B_M^2 - B_I^2} \quad (2)$$

where B is the modified peak full width at half the maximum intensity of XRD patterns, θ is the Bragg angle, λ is the wavelength of the X-ray used, d is the crystallite size, e is the lattice strain, B_M and B_I refer to milled and annealed powders, respectively. Thus, when $B\cos\theta$ was plotted against $\sin\theta$, a straight line was obtained with the slope as e and the intercept as $0.9\lambda/d$. From these, crystallite size, d, and lattice strain, e, were calculated [14].

3. Results and discussion

3.1. Mechanical alloying process

The evolution of the transformations occurring during milling process was performed by X-ray analysis as shown in Fig. 1. According to Fig. 1, the peaks related to raw materials (Al, Ni, Cr and Mo) can be seen in starting materials. After 5 h of milling, the peaks related to Al, Cr and Mo vanished but only Ni peaks remained visible. After 10 h of milling, the Ni peaks shifted to lower angles that can be described by the diffusion of the elements Al, Cr and Mo into Ni structure and the formation of a Ni-based solid solution phase. A Ni_3Al intermetallic compound was formed after 15 h of milling. Lack of superlattice diffraction peaks suggests that the crystalline Ni_3Al phase has a disordered structure. There is no major difference among the peaks of the materials produced after milling of raw materials from 15 to 40 h except broadening of the peaks and decreasing of their intensity.

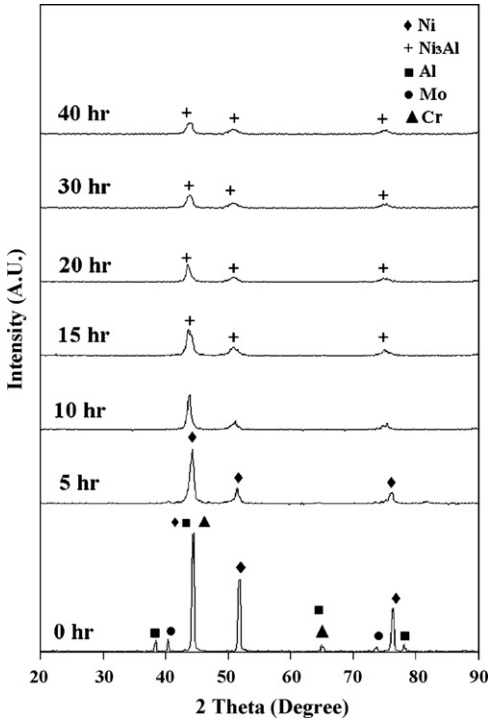

Fig. 1. X-ray patterns of powders of series I after different milling times.

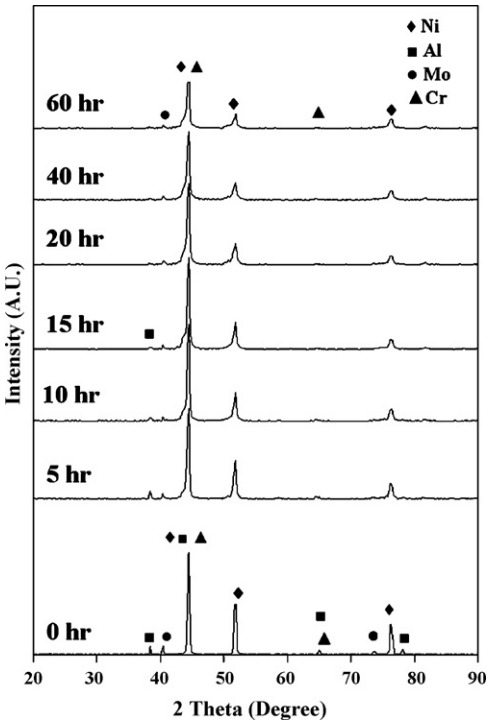

Fig. 2. X-ray patterns of powders of series II after different milling times.

When the milling speed was decreased to 150 rpm in samples of series II, the peaks related to Al were still observed even after milling for 15 h and those related to Cr, Mo and Ni were observed even after 60 h of milling. However, the decreasing peak intensities and broadening peaks were not considerable in the samples of series II, as shown in Fig. 2.

The XRD patterns of samples of series III are presented in Fig. 3. Similar to the results obtained from the samples of series I, the peaks related to Al, Cr and Mo disappeared after 5 h of milling where a solid solution phase containing Ni-based alloying elements formed after 10 h of milling. Prolonged milling up to 15 h led to the formation of a Ni_3Al-based disordered intermetallic phase.

Variations in the crystallite size versus milling time in the samples of series I, II and III are shown in Fig. 4. According to this figure, crystallite size initially decreased sharply with prolonged milling time but it took a decreasing trend for longer milling times. This phenomenon has also been reported by many researchers [14–19]. Finally, with enough longer times, milling was observed to have no considerable effect on crystallite size. It has been established that particle strain increases while particle size decreases at the onset of the milling process when recovery and recrystallization of powder particles occur simultaneously. With prolonged milling times, it is possible to create an equilibrium between the above-mentioned processes so that particle size becomes nearly fixed [20–22]. On the other hand, decreasing of particles size leads to increased energy of the material. Therefore, decreasing particle size is by itself a limiting factor for further decreasing of particle size [23].

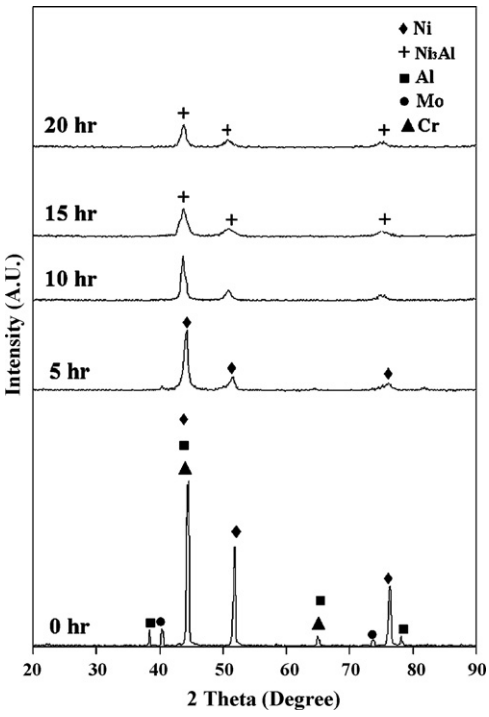

Fig. 3. X-ray patterns of powders of series III after different milling times.

It should be noted that a greater peak broadening due to milling was observed in the samples of series III than in those of series I. This is due to the fact that impacts experienced by and among powder particles, the milling vial, and the balls in dry milling are more intensive than those under wet conditions. Therefore, the particles in samples of series III had a smaller size than those in series I.

Lattice Strain for milled powders of series I, II and III, versus milling time is shown in Fig. 5. The variations in lattice strain in the samples of series III were more intensive than those in series I. But in the samples of series II, variations in lattice strain versus milling time were not considerable due to low energy of impacts.

Variations in the lattice parameter of the milled powders versus milling time are presented in Fig. 6. For the samples of series I and III, lattice parameter of milled powders increased sharply at the onset of milling but its rate of increase considerably decreased over longer milling times. Ball milling had no considerable effect on the lattice parameter in the samples of series II. These events can be described with regard to XRD patterns (Figs. 1–3). Shifting of Ni peaks to lower angles after milling of raw materials for 10 h in the samples of series III is evidence showing the solution of the alloying elements in the Ni lattice. Therefore, the lattice parameter of nickel increases. The

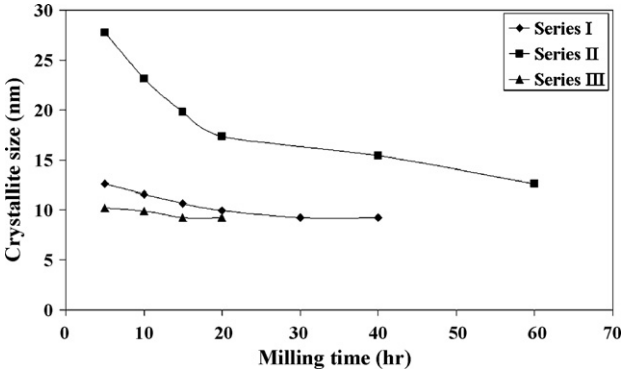

Fig. 4. Variation of crystallite size versus milling time under different conditions.

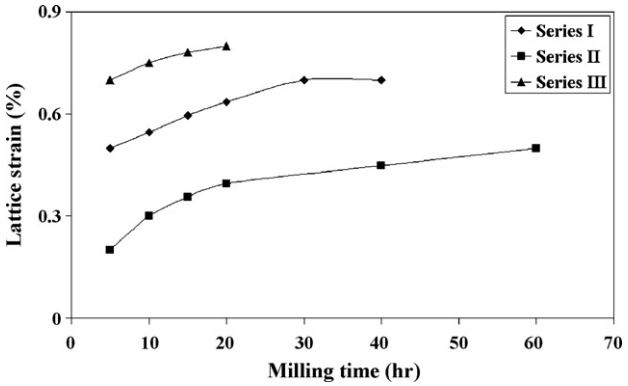

Fig. 5. Variation of lattice strain versus milling time under different conditions.

atomic radius of Al (0.143 nm) and Mo (0.136 nm) are larger than that of Ni (0.125 nm), whereas the atomic radii of Cr (0.125 nm) is almost equal to that of Ni [24]. Therefore, diffusion of Al and Mo atoms into the Ni lattice leads to an increase in the Ni lattice parameter and the transfer of X-ray peaks of Ni to lower angles. According to Fig. 6, in the range of 5 to 10 h of milling in the samples of series I and III, the lattice parameter increased sharply, this is due to the diffusion of the alloying elements into the Ni lattice. This diffusion also led to the formation of a Ni-based solid solution phase after 10 h of milling.

Lattice parameter in the sample of series III after 15 h of milling was less than that in the samples of series I, which is evidence of the lower dissolution of the alloying elements in the Ni lattice in the sample of series III. This may be due to the excessive adhesion of powders to the milling vial and balls during the process. Therefore, a non-homogenate Ni_3Al-based material can be obtained after 15 h of dry milling. According to Fig. 6, this non-homogenate structure transformed to a homogenate one after 20 h of dry milling and the lattice parameter, therefore, reached its relatively fixed quantity.

Table 2
EDX analysis of milled powders of series I and III after different milling times.

Series	Milling time (h)	Element (wt.%)				
		Ni	Al	Cr	Mo	Fe
I	15	82.26	8.09	7.98	1.67	–
	20	82.82	7.82	6.70	1.24	1.42
	30	82.29	7.61	7.16	1.41	1.53
	40	82.08	7.56	6.96	1.58	1.82
III	15	80.61	9.85	7.49	2.05	–
	20	82.30	7.59	7.98	2.13	–

B was not detected.

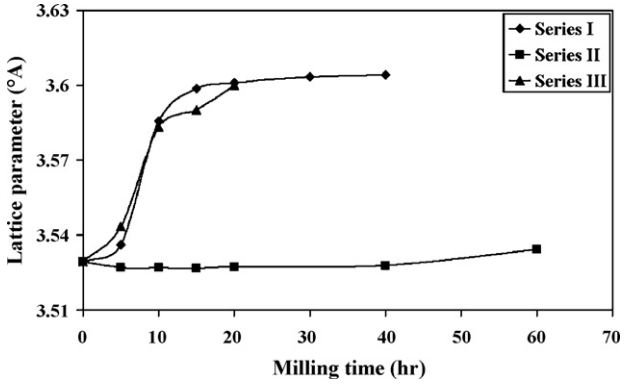

Fig. 6. Variation of lattice parameter versus milling time under different conditions.

Table 3
Comparison of compressive yield strength of the produced alloy with some Ni_3Al-based alloys at room and high temperatures.

Alloys	Temperature (°C)	Yield strength (MPa)	References
Ni_3Al–Cr–Mo–B (hot pressed)	Room temperature	1449	This work
	300	1452	
	600	1492	
	700	1392	
Ni_3Al–Ti–Fe–B (hot vacuum pressed)	Room temperature	820	[25]
	600	1200	
Ni_3Al–Ti–Fe–B (hot vacuum pressed)	Room temperature	750	[25]
	600	1180	
Ni_3Al–B (hot extruded)	Room temperature	420	[25]
	600	850	
Ni_3Al–B (hot extruded)	Room temperature	300	[25]
	600	580	

EDX analysis was used to gain a better understanding of the XRD results obtained for the samples in series I and III, as shown in Table 2. The samples of Series I had a homogenate structure after 15 h of milling with a good agreement with the nominal compositions of alloy (Ni–8.14Al–7.83Cr–1.45Mo–0.01B (wt%)), where after 20 h of milling Fe contamination appeared in EDX analysis due to excessive wearing of the steel vial and balls. Fe contamination increased over prolonged milling times. In the samples of series III milled for 15 and 20 h, Fe contamination was not detected due to the excessive adhesion of powders to the vial and balls. But the chemical composition of 15-h-milled powder under this condition did not have a good homogeneity and showed a considerable difference with the nominal compositions of the considered alloy. A good homogeneity was, however, achieved after 20 h of milling. Therefore, better results can be obtained via wet milling of the starting materials. On the basis of the results obtained powders wet milled for 15 h were selected for densification of the alloy by hot pressing.

3.2. Densification process

The hardness and density of the densificated alloy were 48 HRC and 7.79 g/cm^3, respectively. The compressive yield strength of this alloy compared to some Ni_3Al-based alloys at room and high temperatures [25], is shown in Table 3. It should be noted that the yield strength of Ni_3Al intermetallic compound and alloys with this base changes with temperature in an abnormal manner. In other words, yield strength increases with increasing temperature up to about 600–800 °C due to the change in the sliding system from ⟨1 1 0⟩ {1 1 1} at lower temperatures to ⟨1 1 0⟩ {1 0 0} at higher temperatures. Activation of a new sliding system at higher temperatures leads to facilitated dislocation motions [1–3]. According to Table 3, the alloy produced had very interesting properties.

4. Conclusion

Elemental Ni, Al, Cr, Mo and B powder mixtures with nominal compositions of Ni–8.14Al–7.83Cr–1.45Mo–0.01B (wt%) were mechanically alloyed in a planetary ball mill under different conditions and the alloy produced was densificated to estimate some physical and mechanical properties. The findings of this study can be summarized as follows:

1. After 5 h of milling at a rotating speed of 300 rpm, Al, Cr and Mo peaks vanished and after 10 h of milling, a Ni-based solid solution phase was formed. This structure transformed to a disordered Ni_3Al-based alloy after 15 h of milling under both wet and dry conditions. But a good chemical homogeneity of structure was achieved after 15 and 20 h of milling under wet and dry conditions, respectively.
2. Yield strength of hot pressed powders increased with increasing temperature up to 600 °C.
3. The mechanical properties of the produced alloy were very interesting, especially for high temperature applications.

References

[1] J.H. Westbrook, R.L. Fleischer, Intermetallic Compounds: Structural Applications, vol. 3, John Wiley, New York, 2000.
[2] G. Sauthoff, in: R.W. Chan, P. Hassen, E.J. Kramer (Eds.), Materials Science and Technology: A Comprehensive Treatment, vol. 8, VCH Publishers Inc., New York, 2005, pp. 643–803.
[3] N.S. Stoloff, Int. Mater. Rev. 34 (1989) 153–183.
[4] J.H. Westbrook, R.L. Fleischer, Intermetallic Compounds: Practice, vol. 2, John Wiley, New York, 1994.
[5] Y.V.R.K. Prasad, S. Sasidhara, V.K. Sikka, Intermetallics 8 (2000) 987–995.
[6] S.C. Deevi, V.K. Sikka, Intermetallics 4 (1996) 357–375.
[7] V.K. Sikka, S.C. Deevi, S. Viswanathan, R.W. Swindeman, M.L. Santella, Intermetallics 8 (2000) 1329–1337.
[8] V.K. Sikka, J.T. Mavity, A. Anderson, Mater. Sci. Eng. A 153 (1992) 712–721.
[9] V.K. Sikka, M.L. Santella, J.E. Orth, Mater. Sci. Eng. A 239–240 (1997) 564–569.
[10] S.C. Deevi, V.K. Sikka, Intermetallics 5 (1997) 17–27.
[11] V.K. Sikka, S.C. Deevi, J.D. Vought, Adv. Mater. Processes 6 (1995) 29–31.
[12] S.C. Deevi, V.K. Sikka, C.T. Liu, Prog. Mater Sci. 42 (1997) 177–192.
[13] D. Lee, M.L. Santella, I.M. Anderson, G.M. Pharr, Intermetallics 13 (2005) 187–196.
[14] C. Suryanarayana, Mechanical Alloying and Milling, Marcel Dekker, New York, 2004.
[15] L. Lu, M.O. Lai, S. Zhang, J. Mater. Process. Technol. 48 (1995) 683–690.
[16] L. Lu, M.O. Lai, S. Zhang, Mater. Des. 15 (1994) 79–86.
[17] M.H. Enayati, Z. Sadeghian, M. Salehi, A. Saidi, Mater. Sci. Eng. A 375–377 (2004) 809–811.
[18] S. Benhaddad, S. Bhan, A. Rahmat, J. Mater. Sci. Lett. 16 (1997) 855–857.
[19] X.M. Wang, K. Aoki, T. Masumoto, Mater. Sci. Forum 225–227 (1996) 423–428.
[20] C.C. Koch, Nanostruct. Mater. 2 (1993) 109–129.
[21] J.D. Whittenberger, Proceedings of the International Symposium on Solid State Powder Processing, TMS Pub, 1990, pp. 137–155.
[22] A. Benghalem, D.G. Morris, Acta Metall. Mater. 42 (1994) 4071–4081.
[23] T.G. Nieh, J. Wadsworth, Int. Mater. Rev. 44 (1999) 59–75.
[24] J.F. Shackelford, W. Alexander, Materials Science and Engineering Handbook, CRC Press LLC, 2001.
[25] D. Bozic, N. Ilic, M. Mitkov, M.T. Jovanovic, M. Zdujic, J. Mater. Sci. 31 (1996) 3213–3221.